Impact of mixing state on aerosol optical properties during severe wildfires over the Euro-Mediterranean region

Marwa Majdi, Youngseob Kim, Solène Turquety, Karine Sartelet

Impact of mixing state on aerosol optical properties during severe wildfires over the Euro-Mediterranean region

Marwa Majdi[a,b], Kim Youngseob[a], Solene Turquety[b], Karine Sartelet[a]

[a] CEREA: joint laboratory École des Ponts ParisTech - EdF R&D, Université Paris-Est, 77455 Champs-sur-Marne, France
[b] Laboratoire de Météorologie Dynamique (LMD)-IPSL, Sorbonne Université, CNRS UMR 8539, École Polytechnique, Paris, France

Abstract

The impact of mixing state of particles from biomass burning on aerosol optical properties (aerosol optical depth (AOD) and single-scattering albedo (SSA)) is studied over the Euro-Mediterranean region during the severe fire event in the Balkans between 20 and 31 July 2007, also characterized by high dust concentrations. When the mixing state is resolved in chemistry-transport models, chemical compounds are grouped for computational reasons, and internal mixing is assumed within each group. Up to six groups are de ned here (dust, black carbon, two inorganic groups and two organic groups). The influence of different grouping assumptions is studied here and compared to the influence of the distribution of black carbon (BC) in particles ("pure homogeneous" representation and "core-shell" one), and the influence of modeling the water absorbed by both inorganic and organic compounds. The comparisons of simulated AODs to observations from the surface network AERONET show that AOD is slightly underestimated when aerosol compounds are assumed to be externally mixed and slightly overestimated when they are assumed to be internally mixed. The mixing state

of dust with other compounds, as well as the distribution of BC in particles, strongly influence the optical properties. The impact of the mixing state on AOD is higher than the impact of the distribution of BC in particles, reaching 8-12% on average over the fire regions and 16% in the fire plume. Analysis related to the impact of particle mixing state and BC distribution on SSA shows results similar to AOD. The impact of the mixing state on SSA can reach -8.5% over the fire regions and it is higher than the impact of the BC representation, which is lower than 2%. At the location of fires, water absorbed by inorganics and organics is shown to influence the AOD by about 2%, which is in the lower range of the influence of water on AOD over the region (between 0 and 40%). This low influence of water on AOD during fire is due to assumptions made in the modelling, where most of secondary organic aerosols formed during fires are assumed to be hydrophobic.

Keywords: Aerosol optical properties - mixing state - black carbon - core-shell - hydrophilic - hydrophobic

1 Introduction

Atmospheric aerosols strongly affect the atmospheric radiative budget due to their direct, semi-direct and indirect interactions with solar radiation. The direct and semi-direct effects are due to the radiative properties of particles (Chylek and Coakley, 1974) which can either absorb or scatter radiation (Haywood and Boucher, 2000; Jacobson, 2002). The indirect effect corresponds to the change of cloud properties due to the presence of particles that may serve as cloud condensation nuclei (CCN) (Twomey, 1977; Koehler

et al., 2009). Absorbing aerosols also modify cloud properties by increasing the local temperature which reduces the relative humidity and inhibits the formation of clouds. This is called the semi-direct aerosol effect (Hansen et al., 1997). The aerosol optical depth (AOD), the single scattering albedo (SSA), the asymmetry parameter and the scattering phase function are the most important and commonly used parameters to describe the aerosol interactions with radiation. Several studies showed the important effects of aerosols on climate (Jacobson, 2002; Bond et al., 2013; Pascal et al., 2013). Estimating climate forcing remains, however, uncertain because of the large uncertainties on the simulation of aerosols and their optical properties (OP) (Lesins et al., 2002).

Particles are composed of different compounds (dust, insoluble and water soluble organics, inorganics and black carbon). The mixing state of particles, i.e. the way compounds co-exist in different particles (total or partial mixing) may affect aerosol OP.

For computational efficiency reasons, the aerosol mixing state is usually not resolved but represented in a simplified way in 3D models, in lagrangian and eulerian models (such as climate or chemistry-transport models CTMs) (Riemer et al., 2019). Two different approaches are commonly used (Jacobson et al., 2000). One approach is the external-mixing approach: the different chemical compounds are assumed to be in separate particles, and there is no physical nor chemical interaction between the different particle compounds. The other approach is the internal-mixing approach: the different chemical compounds are assumed to be mixed in particles, leading to the formation of particles that all have the same chemical composition for a given particle size.

In the real atmosphere, the mixing state is expected to be between these two extremes (Lesins et al., 2002): aerosols are neither externally nor internally mixed, but they have different mixing states (Deboudt et al., 2010; Healy et al., 2012; Zhu et al., 2016; Freney et al., 2018). For African dust, Deboudt et al. (2010) use Transmission Electron Microspectrometry (TEM) and Raman microscopy analyses to show that particles are mostly externally mixed.

When particles are emitted as an external mixture, several processes in the atmosphere (such as coagulation, evaporation/condensation, scavenging, aqueous or intra-particle reactions) convert the external mixture to an internal one (Lesins et al., 2002). In 3D eulerian chemistry-transport models, the internal-mixing approach is often used (e.g. CHIMERE (Menut et al., 2013), CMAQ (Carlton et al., 2010), Polyphemus (Sartelet et al., 2012), EURAD (Li et al., 2015), MOCAGE (Guth et al., 2015)). In the external-mixing approach, for simplicity, some models, such as lagrangian models, neglect coagulation and consider only condensation/evaporation, which may be the most crucial process to model aerosol mass. In the first lagrangian and eulerian models of Kleeman et al. (1997) and Kleeman and Cass (2001), particles are assumed to be externally-mixed, and a specific aerosol distribution is associated to each emission source. To represent the particle mixing-state independently of sources, Jacobson et al. (1994) and Luand Bowman (2010) separated the mixed particles from particles of pure chemical compounds. More recent models allow the mass fraction of any chemical compound to be discretized into sections, similarly to the size distribution (Jacobson, 2002; Oshima et al., 2009; Dergaoui et al., 2013; Zhu et al., 2015). Using the Size Composition Resolved Aerosol Model

(SCRAM) that simulates the particle mixing state and solves the aerosol dynamic evolution considering the processes of coagulation, condensation/evaporation and nucleation (Zhu et al., 2015), Zhu et al. (2016) show that the difference in terms of AOD caused by the mixing-state assumption can be as high as 7.25% for the weekly averaged AOD and 72.5% for the hourly averaged AOD over the Greater Paris area during summer. For biomass burning, different studies show that the particle size and mixing state influence significantly the direct radiative effect (Amiridis et al., 2009; Lack et al., 2012; Matsui et al., 2018). For example, Lack et al. (2012) found that internal mixing of black carbon (BC), organic matter and ammonium nitrate enhances absorption by up to 70%.

The mixing state of particles influence aerosol OP because it influences the composition of particles, which in turn influences their scattering and absorption properties, as well as phase function. This influence is due to several factors: the mixing state and the morphology of BC (Andersson and Kahnert, 2016), as well as the absorption of water by inorganic and organic compounds of particles.

Concerning the Mediterranean in summer, Chrit et al. (2017) showed that 64% of organic carbon at Cap Corsica is soluble. Zhu et al. (2016) showed clearly that, over Greater Paris in summer, AOD differences are strongly sensitive to differences in aerosol water concentrations. They found that the mixing state can lead to differences in water concentrations of about 80%, leading to differences in AOD of about 72%.

In addition to the mixing state, the aerosol OP are influenced by the distribution of BC inside the particles. Secondary compounds, which are formed in the atmosphere, may condense onto BC, which is directly

emitted and inert. The distribution of BC in the particles may be represented as a "pure homogeneous" distribution (BC is well mixed in particles) or as a "core- shell" one (it is assumed to be located at the core of particles). Although BC contributes to less than 5% of the aerosol mass loading, it has an important impact on the OP of the aerosol mixture (Lesins et al., 2002). Matsui et al. (2018) found large uncertainties in BC radiative effects linked to the coating of BC by other compounds. Several studies (Jacobson, 2001; Chandra et al., 2004; Satheesh et al., 2006; Dey et al., 2008; Klingmuller et al., 2014; Péré et al., 2014; Gurci et al., 2015) showed that the core-shell distribution is more realistic, and that it leads to significant differences in aerosol OP compared to the homogeneous one. Andersson and Kahnert (2016) found that a better description of particle morphology and mixing state in a CTM strongly affects the aerosol OP and has the same effects as aerosol-microphysical processes. The impact of the aerosol mixing state may be especially large over the Euro-Mediterranean region, because it is strongly affected by aerosols from a variety of sources: dust, sea salt, anthropogenic and biogenic sources (Monks et al., 2009; Nabat et al., 2015; Rea et al., 2015; Chrit et al., 2017). Further- more, wild res are an important source of aerosols in the Euro-Mediterranean region (Turquety et al., 2014). Although they are sporadic, they contribute significantly to the atmospheric aerosol loading (Barnaba et al., 2011; Rea et al., 2015), especially during summer.

This paper aims at estimating and comparing the impacts of the aerosol mixing state and the core-shell distribution of BC on aerosol OP (AOD and SSA) during the intense wild re episodes of summer 2007 over Balkan. Different grouping methods of aerosol chemical compounds are compared to

define an optimal method for 3D modeling.

The approach presented here consists in computing AOD and SSA at 550 nm, from the reference Polyphemus simulation of Majdi et al. (2019), under different particle mixing-state scenarios and different particle core treatments.

The work is structured as follows. Section 2 details the method used to compute AOD and SSA, as well as the sensitivity tests performed. Sections 3 presents the statistical evaluation of the model performance for the different scenarios. The impact on AOD and SSA of different mixing state and BC core-shell distribution scenarios, as well as the impact of absorption of water by inorganic and organic compounds are discussed in section 4. Section 5 presents the conclusions and the perspectives of this study.

2 Computation of the aerosol optical properties for different mixing states and core-shell scenarios

2.1 Model description

In this study, the chemistry-transport model (CTM) Polair3D/Polyphemus (Mallet et al., 2007; Sartelet et al., 2012) is used to simulate gas and aerosol concentrations during the summer of 2007 over the Euro-Mediterranean region. The simulation setup and domain are detailed in Majdi et al. (2019).

Two domains are considered: the nesting domain covers Europe and North Africa and the nested one over the Mediterranean. The spatial resolution used from the nesting and nested domains are $0.5^{\circ}\times0.5^{\circ}$ and $0.25^{\circ}\times0.25^{\circ}$ respectively. 14 vertical level are used for both domains from ground to 12 km. The summer 2007 was marked by intense re events over the Euro-Mediterranean region. The event that occured mainly in Balkan and East-

ern Europe (20-31 July 2007) is simulated here. Different input data are used. The European Centre for Medium-Range Weather Forecasts (ECMWF: ERA-Interim) provides the meteorological fields. The global chemistry transport model MOZART-GEOS5 6 hourly simulation outputs (Emmons et al., 2010) are used as boundary conditions of the nesting domain. Anthropogenic emissions are obtained from EMEP (European Monitoring and Evaluation Programme; http://www.emep.int) inventory for 2007.

Biogenic emissions are estimated with the the Model of Emissions of Gases and Aerosols from Nature (MEGAN-LHIV, Guenther et al. (2006)). The parameterization of Monahan (1986) is used for sea-salt emissions.

Dust emissions are calculated using the soil and surface database of Menut et al. (2013) with the spatial ex- tension of potentially emitted area in Europe of Briant et al. (2017). As described in Majdi et al. (2019), the daily re emissions are estimated using APIFLAME fire emission model v1.0 (Turquety et al., 2014). Concerning chemical and aerosol modelling, the gas-phase chemical mechanism used in Polair3D/Polyphemus is the Carbon Bond 05 model (CB05) (Yarwood et al., 2005), modified to model secondary organic aerosol (SOA) formation, as detailed in Kim et al. (2011) and Couvidat et al. (2012). The aerosol dynamics (coagulation, condensation/evaporation) is modeled using the Size REsolved Aerosol Model (SIREAM) (Debry et al., 2007). The size distribution is discretized with 5 sections between 0.01 μm and 10 μm, and the internal-mixing assumption is made. The particle compounds are dust, black carbon, inorganics (ammonium, sulfate, nitrate, sodium, chloride) and organics from biogenic precursors (isoprene, monoterpenes, sesquiterpenes) and anthropogenic or biomass burning precursors (toluene, xylene, intermediate and semi

volatile organic compounds). The partitioning between gas and particles is done assuming bulk equilibrium, using a thermodynamic equilibrium model for multiphase multicomponent inorganic aerosols (ISORROPIA) (Nenes et al., 1998) for inorganics and using the Secondary Organic Aerosol Processor (SOAP) (Couvidat and Sartelet, 2015) for organics. For organics, the oxidation of biogenic and anthropogenic precursors leads to the formation of surrogate compounds, which partition between the gas and the particle phases depending on their affinity to water. They are either hydrophobic (partition onto the organic phase made of hydrophobic compounds) or hydrophilic (partition onto the aqueous phase made of inorganics and hydrophilic organic compounds).

2.2 Aerosol optical properties

The AOD and SSA at a given wavelength (λ), are calculated as the integral of the extinction and backscattering coefficients respectively, through the atmospheric column (equations 1 and 2):

$$\mathrm{AOD}(\lambda) = \int_{z_g}^{n_z} \beta_{ext}(\lambda, z)\, dz \qquad (1)$$

$$\mathrm{SSA}(\lambda) = \frac{\int_{z_g}^{n_z} \beta_{sca}(\lambda, z)\, dz}{\mathrm{AOD}(\lambda)} \qquad (2)$$

where n_z is the altitude at the top of the atmosphere and z_g is the altitude at the ground level.

The algorithm used here to compute AOD and SSA is detailed in Tombette et al. (2008) and Zhu et al. (2016). The extinction and backscattering coefficients (β_{ext} and β_{sca}) are a function of the particle size, wavelength and Aerosol Complex Refractive Index (m) (ACRI which is computed from the Complex Refractive Index (CRI) of each chemical species). The CRI describes the ability of a chemical species to scatter or absorb radiation (Hess et al., 1998). They are taken from the OPAC software package (Optical Properties of Aerosols and Clouds, Hess et al. (1998)), and displayed in Table 1.

Table 1: CRI of simulated compounds at $\lambda = 550$ nm.

Model species	OPAC species	Real	Imaginary
Nitrate	water soluble	1.53	-6×10^{-3}
Ammonium	water soluble	1.53	-6×10^{-3}
Sulfate	sulfate	1.43	-10^{-8}
Sodium	sea salt	1.43	-10^{-8}
Chlorate	sea salt	1.43	-10^{-8}
Black Carbon	soot	1.75	-4.4×10^{-1}
Mineral Dust	mineral	1.53	-5.5×10^{-3}
Primary Organics	insoluble	1.53	-8.0×10^{-3}
Secondary Organics	insoluble	1.53	-8.0×10^{-3}

Once the ACRI value (m) for each particle composed of several chemical components is computed, the extinction and back scattering coefficients are computed using the Mie code (Mie, 1908) of Mishenko et al. (1999). The computation of ACRI for each particle depends on the assumption made on the mixing state of the chemical compounds.

Assuming that particles are spherical, and that the particles are discretized in n_{bin} size sections with n_c different possible particle compositions, then for each vertical level z, the extinction and the scattering coefficients are computed following equations 3 and 4 respectively:

$$\beta_{ext}(\lambda, \mathrm{z}) = \sum_{\mathrm{c}=1}^{\mathrm{n_c}} \sum_{\mathrm{i}=1}^{\mathrm{n_{bin}}} \frac{\pi}{4} d_{\mathrm{wet}}(\mathrm{i}, \mathrm{z}, \mathrm{c})^2 \, Q_{ext}(\mathrm{i}, \mathrm{z}, \mathrm{c}) \, N(\mathrm{i}, \mathrm{z}, \mathrm{c}) \qquad (3)$$

$$\beta_{sca}(\lambda, z) = \sum_{\mathrm{c}=1}^{\mathrm{n_c}} \sum_{\mathrm{i}=1}^{\mathrm{n_{bin}}} \frac{\pi}{4} d_{\mathrm{wet}}(\mathrm{i}, \mathrm{z}, \mathrm{c})^2 \, Q_{sca}(\mathrm{i}, \mathrm{z}, \mathrm{c}) \, N(\mathrm{i}, \mathrm{z}, \mathrm{c}) \qquad (4)$$

where N(i,z,c) and d_{wet}(i,z,c) are respectively, the number and wet diameter of particles in size section i and composition c.

In the case of the internal-mixing approach, the AOD and SSA are calculated in the same way as for the external-mixing approach by assuming that the number of composition n_c is equal to 1, as all compounds in each size section are mixed.

2.3 Mixing hypothesis

Optical properties calculations are made as a post-processing step after the CTM simulation, considering 6 groups of aerosols. Within each group, compounds are assumed to be internally mixed. Species are grouped according to their sources (e.g. dust emissions, BC from combustion...) and their affinity with other compounds. Inorganics (nitrate, ammonium, sulfate) are grouped together, because of their anthropogenic origins, while

sodium and chloride form a different group because of their sea-salt origin. Hydrophilic and hydrophobic organics are separated into two groups, because hydrophilic/hydrophobic compounds may condense more easily on hydrophilic/hydrophobic organic particles than on hydrophobic/hydrophilic ones respectively. In summary, the following groups are considered: anthropogenic hydrophilic inorganics (InorgAnt), sea-salt hydrophilic inorganics (InorgSS), organic hydrophilic (Hydrophilic Org), organic hydrophobic (Hydrophobic Org), black carbon (BC) and dust (DUST). Figure 1 presents the mean proportion of each group in the composition of simulated PM_{10} concentrations. Each group has a large contribution: dust (33.4%), hydrophobic organics (22.4%) and anthropogenic inorganics (19.5%), hydrophilic organics (13.1%) and sea-salt inorganics (9.5%). The proportion of BC is lower (2.1%) than the other groups. Only water absorbed by inorganics is considered here at first. It is therefore affected to the inorganic group. Although this simplifying assumption may potentially minimize the impact of the mixing state; the impact of water is studied later in section 4.

2.3.1 Mixing-state assumption

Using the groups de ned above, different mixing-state scenarios are considered for the calculation of optical properties as shown in Figure 2:

- Scenario 1: Internal mixture (Figure 1-a). All chemical groups are mixed in the particles.

- Scenario 2: External mixture (Figure 1-b). The different chemical groups are in different particles and they do not mix.

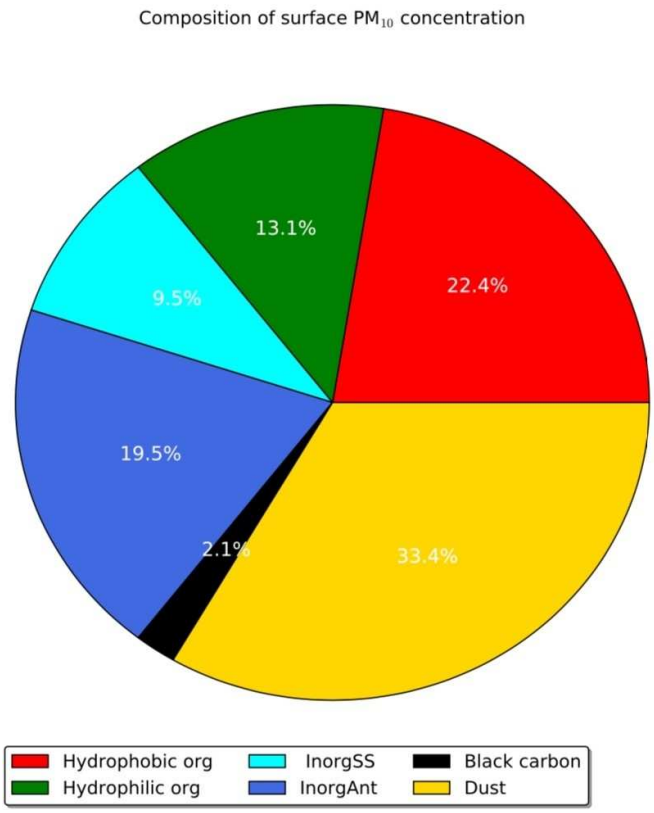

Figure 1: Mean composition of surface PM_{10} concentration during the simulation over the Euro-Mediterranean region.

- Scenario 3: All chemical groups are internally mixed, except dust. Dust, which originates mostly from mineral emissions, may not be mixed with anthropogenic and re emissions (Deboudt et al., 2010).

- Scenario 4: All hydrophilic groups (organics and inorganics) are internally mixed in particles. Dust and BC are not mixed. Because wildfires emit large quantities of BC and hydrophobic organics (Majd

et al., 2019), BC and hydrophobic organics are assumed to be internally mixed.

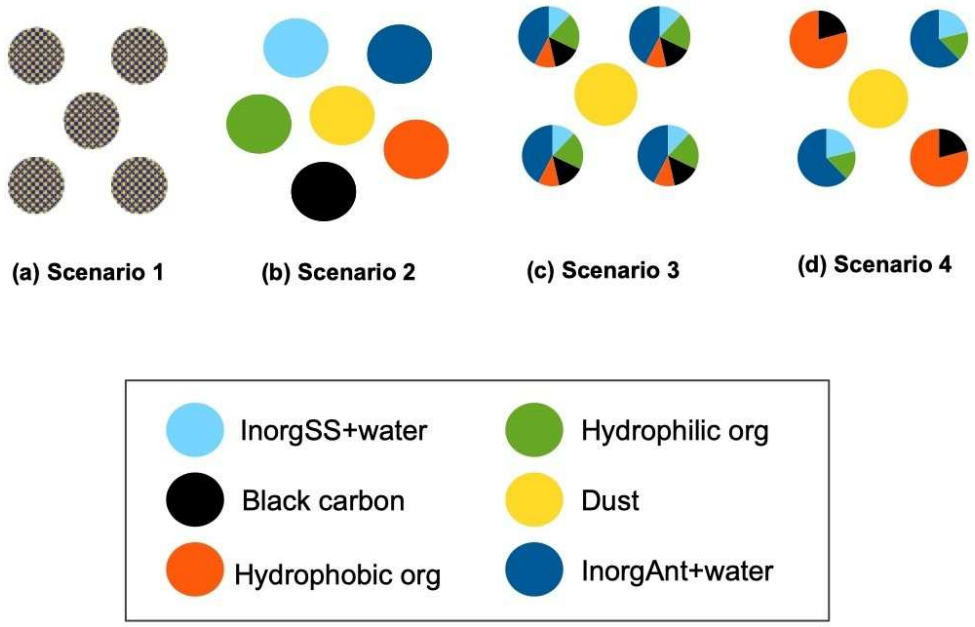

Figure 2: The different mixing-state scenarios considered in this study

2.3.2 Core-shell distribution

BC is assumed either to be homogeneously mixed in particles, or to be as a core. In the homogeneous hypothesis, the different aerosol compounds are well-mixed in each size bin. According to Tombette et al. (2008), the ACRI is calculated from the refractive indexes of pure species using the volume averaged procedure (Lesins et al., 2002).

In the core-shell hypothesis, BC constitutes a non-mixed core at the center of each BC-containing particle. In that case, all other components (hydrophilic

organic compounds, inorganic compounds, dust and hydrophobic inorganic compounds) are well-mixed in the shell. Previous studies have stressed the influence of the core-shell representation on aerosol optical properties (Jacobson et al., 2000; Lesins et al., 2002; Bond et al., 2013). This sensitivity is explained by the fact that coating on an absorbing core enhances light absorption (Khalizov et al., 2009). The effect is more significant when the core is more absorbing (Lesins et al., 2002), as in the case of BC. According to Hess et al. (1998), BC has the largest imaginary part in the CRI, implying that BC is the highest absorbing component in the visible. If BC is assumed to be a non-mixed core at the center of particles, the ACRI (which is the square root of the dielectric constant) is computed using the Maxwell-Garnett approximation (Maxwell Garnett, 1904), as detailed in Tombette et al. (2008).

2.4 Sensitivity tests

The calculation of AOD and SSA at 550 nm is conducted under the different mixing-state and core-shell treatment scenarios. Table 2 summarizes the assumptions used in the different sensitivity tests. Scenarios 1 to 4 correspond to the mixing states described in Figure 2. The comparisons of the OP computed using these different scenarios will allow us to determine the number of groups required in simulations resolving the mixing states.

Scenario 1 assumes that all groups are internally mixed and BC is homogeneously mixed in the particles. Scenario 2 is conducted to assess the maximum impact of the mixing-state hypothesis: in opposition to scenario 1,

all chemical groups are assumed to be externally mixed. To assess the impact of a more realistic mixing-state hypothesis, some chemical groups are mixed in Scenarios 3 and 4, but dust is kept externally mixed. In scenario 3, all chemical groups (Inorg, Hydrophilic Org, Hydrophobic Org, BC) except dust is mixed. In scenario 4, dust is kept externally mixed, but hydrophilic groups are mixed (inorganics and hydrophilic organics), while BC is mixed with hydrophobic organics. The sensitivity to the core-shell treatment is conducted in scenario 5. Scenario 5 is similar to the scenario 1, but BC is treated as a core instead of being homogeneously mixed with other particles. Scenario 5 corresponds to the setup used previously in the study of Majdi et al. (2019). To test the influence of water content on aerosol optical properties, two variations of scenario 2 are studied. Although only the water absorbed by in- organics is considered in scenario 2, in "scenario 2-with-water", the water absorbed by the different chemical groups are computed, using ISORROPIA for inorganics and SOAP for organics. In contrast, in "scenario2-without-water", the water absorbed by the different compounds is not considered.

Table 2: Summary of the assumptions used to simulate aerosol optical properties in the different sensitivity tests.

Sensitivity test	Mixing state	Number of composition	Core-shell treatment	Core com-position
Scenario 1	Internal mixing	1 (all groups are mixed)	No	
Scenario 2	External mixing	6 (all groups are unmixed)	No	
Scenario 3	Partial mixing	2 (all groups are mixed except dust)	No	
Scenario 4	Partial mixing	3 (dust, hydrophilic com-pounds, hydrophobic com-pounds and BC)	No	
Scenario 5	Internal mixing	1 (all groups are mixed)	Yes	BC

3 Statistical evaluation of the model performance

3.1 Observations and comparison method

AOD level 2.0 data (at 550 nm) from the AERONET (AErosol RObotic NETwork) ground-based network of sun photometers (Holben et al., 1998) are used. The uncertainty on AOD is estimated to be less than 0.02 (Holben et al., 2001). In this study, seven AERONET stations (the closest stations to regions where re contribution is higher than 50%) are used to evaluate t h e model performance statistically, as in Majdi et al. (2019).

A set of statistical indicators are used for the comparison of model simulations to surface measurements: the root mean square error (***RMSE***), the correlation coefficient (***R***), the mean fractional bias (***MFB***) and the mean

fractional error (***MFE***). These are defined as:

$$RMSE = \sqrt{\frac{1}{\mathrm{n}}\sum_{\mathrm{i}=1}^{\mathrm{n}}(c_\mathrm{i} - o_\mathrm{i})^2} \tag{5}$$

$$R = \frac{\sum_{\mathrm{i}=1}^{\mathrm{n}}(c_\mathrm{i} - \bar{c})(o_\mathrm{i} - \bar{o})}{\sqrt{\sum_{\mathrm{i}=1}^{\mathrm{n}}(c_\mathrm{i} - \bar{c})^2}\sqrt{\sum_{i=1}^{n}(o_\mathrm{i} - \bar{o})^2}} \tag{6}$$

$$MFB = \frac{1}{\mathrm{n}}\sum_{\mathrm{i}=1}^{\mathrm{n}}\frac{c_\mathrm{i} - o_\mathrm{i}}{(c_\mathrm{i} + o_\mathrm{i})/2} \tag{7}$$

$$MFE = \frac{1}{\mathrm{n}}\sum_{\mathrm{i}=1}^{\mathrm{n}}\frac{\mid c_\mathrm{i} - o_\mathrm{i} \mid}{(c_\mathrm{i} + o_\mathrm{i})/2} \tag{8}$$

with o_i the observed concentration at time and location i, c_i the corresponding modeled concentration and n the number of data.

Boylan and Russel (2006) proposed for PM that a model performance criterion (level of accuracy acceptable for standard modeling applications) is met when MFE $\leq +75\%$ and MFB is within $\pm$ 60%, and a model performance goal (level of accuracy considered to be close to the best a model can be expected to achieve) is met when MFE $\leq$ 50% and MFB is within $\pm$30%. In the following, the MFBs and MFEs are computed at each station and averaged over all stations.

3.2 Model evaluation

Table 3: Statistics of model-to-measurement comparisons for mean daily AOD at 550 nm during the re event from 20 July to 31 July 2007.

Sensitivity test	Mean observed AOD	Mean simulated AOD	Correlation (%)	MFB (%)	MFE (%)
Scenario 1	0.28	0.28	70	8	29
Scenario 2	0.28	0.25	70.3	-7	30
Scenario 3	0.28	0.25	70.5	-6	29
Scenario 4	0.28	0.25	70.4	-6	29
Scenario 5	0.28	0.27	71.1	3	30

The statistical evaluation of the simulations during the fire event from 20 July to 31 July 2007, is presented in Table 5.3 for the AOD at 550 nm. The mean AOD is well reproduced by the model for all scenarios. The model performance and goal criteria are always met. The model-to-measurements correlations are high and range between 70 and 71% for all scenarios. The MFEs are similar for all scenarios (29% to 30%), but the MFBs differ depending on the scenarios. The AOD is underestimated by up to 7% in the scenarios where the particles are partially or externally mixed (scenarios 2, 3 and 4), and it is overestimated by up to 8% in the scenarios where the particles are internally mixed (scenarios 1 and 5).

The core distribution of black carbon enhances the black carbon absorption by a factor between 1.1 and 1.2, which is slightly lower than the en-

hancement modelled by Curci et al. (2019), but in the range suggested by Bond and Bergstrom (2006).

4 Sensitivity analysis

4.1 Spatial impact of the mixing state and core-shell distribution

To better quantify and compare the impact of different mixing states and core treatment assumptions on AOD and SSA, sensitivity studies are conducted over the Euro-Mediterranean region between 20 and 31 July. Figures 3 and 4 show the mean AOD and SSA respectively (left upper panel) from scenario 5, which is the reference simulation in Majdi et al. (2019), over the Euro-Mediterranean region between 20 and 31 July 2007, and the impact of the mixing state and core treatment of particles. The mean AOD is large in the region of wild res, between 0.5 and 0.6, and above 0.3 in the fire plumes. The SSA stays between 0.93 and 0.94 over the regions impacted by fires and in the fire plumes. It is higher and reaches 0.98 in the western part of the domain, where dust has a large influence.

The impact of the mixing state is shown in the right upper panel of Figures 2 and 3 for AOD and SSA respectively. It corresponds to the relative difference between scenario 2 (external mixing) and 1 (internal mixing). For AOD, the impact is between -8% and -12% close to the fire regions Balkans) and it reaches ∼-16% further downwind in the re plume. For SSA, the impact is lower. It is between 2% and 8% in the re regions.

Amongst the mixing-state scenarios, scenario 2 (all groups externally mixed) is the most different from the scenario 1 (all groups internally mixed).

The impact of partial mixing between different groups is lower, especially for AOD. The comparison between the scenarios 3 and 2 (left middle panel of Figures 2 and 3) shows the impact of considering the mixing of groups other than dust. This mixing leads to a slight increase of AOD by +1.8% in the fire plume, up to +1.4% above the fire region, and to a decrease of SSA of up to -4%. The impact of assuming that BC and hydrophobic organic compounds are mixed and that inorganics are mixed with hydrophilic organic compounds is similar to the impact of considering the mixing of groups other than dust (right middle panel of Figures 3 and 4). It is between +1.4% and +1.8% for AOD and up to -3% for SSA. The partial mixing of groups other than dust has a low influence on both AOD and SSA. However, this influence may be under-estimated here, because water absorbed by organics is not modelled. The impact of aerosol water concentrations on the aerosol optical properties is discussed in section 4.2.

The impact of the core treatment of BC is shown in the lower panels of Figures 3 and 4 for AOD and SSA respectively. This impact is lower than the impact of the mixing state. Considering BC as core instead of homogeneous leads to a decrease of AOD between -2 and -4% above the fire region and up to -8% in the fire plume. Similar results were found above Greater Paris by Zhu et al. (2016).

4.2 Impact at the location of fire

To understand the differences in AOD and SSA values between the different scenarios and their relation to fires, the temporal evolution of AODs is first studied, followed by the variations of the extinction

coefficient (β_{ext}) between the scenarios. The variations of the backscattering backscattering coefficient (β_{sca}) is similar to those of the extinction coefficient and it is therefore not shown.

4.2.1 Temporal impacts of the mixing state and core-shell distribution

Figure 5 shows the time evolution of AOD at 550mn from scenario 5 at point A between 20 and 31 July 2007. AOD is large mainly between 25 and 28 July. It can reach up to 1.4 on 26 July during the severe wild res. At the beginning of the simulation, when dust concentrations are the highest (Figure 5), the influence of the mixing state is large (-22% difference between scenarios 1 and 2), but the influence of the core-shell assumption is low (less than 3% difference in absolute value between scenarios 1 and 5). However, as the res develop, the core-shell assumption becomes more important (up to -18% difference), and the mixing-state assumption less important (-12%).

4.2.2 Influence of the different groups

Figure 6 shows β_{ext} for each scenario at point A where res occurred, at midday, on 25 July 2007 (fire peak) and on 31 July 2007 (end of the fire episode). Results are shown at the vertical level between 1000 m and 1500 m where re emissions are injected. The coefficients are integrated over the five diameter bins, but the contribution of the different particle types is shown (each particle type is made of one or several groups depending on the scenario).

On both days (25 and 31 July 2007), β_{ext} is higher for scenarios assuming internal-mixing than for those assuming external mixing. On 25 July 2007, as shown by the β_{ext} of the external-mixing scenario (scenario 2), dust is the

group most influencing AOD and SSA, followed by hydrophobic organics, inorganics, BC and hydrophilic organics. On 31 July 2007, the influence of dust is lower and the influence of other groups is higher, especially for hydrophobic organics, BC and anthropogenic inorganics. This is due to the emission by fires of BC and precursors of hydrophobic organics and inorganics (ammonia), leading to a lower dust contribution to PM_{10} composition on 25 July than 31 July 2007 (Figure 7).

For AOD, the highest β_{ext} values are found in scenario 1, for which particles are internally mixed and the homogeneous treatment of BC is considered. Because BC is the highest light-absorbing compound, considering BC mixed with other particles leads to higher absorption efficiency and a higher β_{ext}, as shown by the difference in β_{ext} between scenarios 2 and 1, and between scenarios 2 and 3. Similarly, considering BC homogeneously mixed in the particles leads to higher β_{ext}, as shown by the difference in β_{ext} between scenarios 5 and 1. The partial mixing of groups other than dust has a low influence on β_{ext} on both days.

4.1.1 Influence of water

To test the influence of water content on optical properties, the variation of β_{ext} between scenario 2-with-water and scenario 2-without-water are studied, at point A at midday on 25 July at the vertical level between 1000 and 1500m. Figure 8 shows that β_{ext} value in the scenario 2-with-water is higher than in the scenario 2-without-water. β_{ext} values are higher by about 15% for hydrophilic compounds (inorganics and hydrophilic organics) when water is considered. Although the impact of water on β_{ext} values and AOD is important, it is limited to two percents when the

whole particle distribution is considered, because a large fraction of compounds is hydrophobic (dust and hydrophobic organics). In case of wild res, a large part of organic compounds is made of intermediate and semi volatile organic compounds,

which are assumed by default to be hydrophobic in the model (Majdi et al., 2019). This contribution of water absorbed by inorganics and organics to AOD during the re event is low compared to the contribution over the computational domain, which ranges between 0% and 40% at midday on 25 July. This highlights the importance to consider the water absorbed not only by inorganics but also by the hydrophilic organics. For wildfires, the hydrophobic assumption of SOA may not be realistic, and it is therefore desirable to better characterize the hydrophilic properties of SOA formed during wildfires.

5 Conclusion

Aerosols from biomass burning strongly influence the radiative balance. Since estimating their climatic forcing remains uncertain partly because of the optical properties of aerosols that depend on their composition as well as their mixing state, a sensitivity analysis was conducted to estimate the impact of the aerosol mixing state on aerosol optical properties (AOD and SSA) over the Euro-Mediterranean region during the severe re event in Balkans (from 20 to 31 July 2007). Aerosol concentrations were computed using the air-quality model Polyphemus, and different assumptions (leading to different scenarios) on the mixing state of particles, the core-shell distribution of BC and the calculation of water were made when computing the optical properties. The computed

AOD compared well to background AERONET surface observations, with high correlations and low errors. The bias differs depending on the scenarios: the AOD was underestimated by up to 7% in the scenarios where the particles were partially or externally mixed, and it was overestimated by up to 8% in the scenarios where the particles are internally mixed.

This study points out the strong influence of the mixing state of dust and the core-shell distribution of BC in particle on optical properties. Because BC is the highest absorbing compound, AODs are lower when BC is assumed to be at the core of particles than when it is homogeneously mixed. Similarly, AODs are lower when BC and dust are externally mixed, i.e. when they are in different particles than the other compounds, than when they are internally mixed. The impact of the mixing-state assumption (internal or external) on AOD is higher than the impact of the treatment of BC in particles (core or homogeneous).

It reaches 8 12% over the re region and 16% in the fire plume for the mixing-state assumption, and -4% over the re regions and -8% in the fire plume for the BC treatment assumption. Similar results are found for SSA. The impact of the aerosol mixing-state on SSA (up to -8.5%) is higher than the impact of core-shell treatment (lower than 2%). This shows that the choice of the mixing-state approach is of major importance for AOD modeling and has consequences on the calculation of their radiative impact and on model evaluation against remote sensing measurements. The influence of the mixing state is mostly due to dust in this work. The mixing state of compounds other than dust has a limited impact on optical properties. It is lower than 2% for AOD and lower than 4% for SSA.

However, this influence may be under-estimated here, because water absorbed

by organics is not taken into account in the calculations presented above.

To better understand the impact of water content on optical properties, sensitivity tests are conducted in this work and highlight that taking into account water from hydrophilic organics enhances β_{ext} values and thus AOD. Although the sensitivity of AOD to aerosol water content is shown to vary between 0 and 40% in the Mediterranean at the peak of the fire event, the sensitivity is estimated to be lower than 2% at the location of the fire event, because most the organic compounds from res are assumed to be hydrophobic in the model. A better characterization of the hydrophilic properties of SOA is required to confirm this influence.

This work shows that the representation of the mixing state of particles influences the optical properties of aerosols during wildfires, even more than the distribution of black carbon in particles. When the mixing state of particles is resolved in chemistry-transport models (see Zhu et al. (2015)), it cannot be resolved for all chemical compounds, because of high computational cost. Compounds need to be grouped. Different mixing-state configurations and grouping are considered here. During strong wildfires with high dust concentrations, as in the event of this study, only two groups (dust and a group consisting of other compounds) may be necessary to accurately represent aerosol optical depth (2% difference with different grouping of other compounds) and single scattering albedo (4% difference). Further work should involve resolving the mixing state of dust explicitly in the chemistry-transport simulation with a detailed discretization of the composition. Measurements, for example using scanning or transmission electron microscopy, would also be useful to verify the mixing states that

co-exist in the atmosphere during such event.

Acknowledgements

CEREA is a member of the Institut Pierre-Simon Laplace (IPSL). This research was partially funded by a PhD grant from École des Ponts ParisTech.

References

Amiridis, V., Balis, D., Giannakaki, E., Stohl, A., Kazadzis, S., Koukouli, M., Zanis, P.. Optical characteristics of biomass burning aerosols over Southeastern Europe determined from UV-Raman lidar measurements. Atmos Chem Phys 2009; 9:2431 2440. doi:10.5194/acp-9-2431-2009.

Andersson, E., Kahnert, M.. Coupling aerosol optics to the MATCH (v5.5.0) chemical transport model and the SALSA (v1) aerosol microphysics module. Geosci Model Dev 2016; 9:1803 1826. doi:10.5194/gmd-9-1803-2016.

Barnaba, F., Angelini, F., Curci, G., Gobbi, G.P.. An important fingerprint of wildfires on the European aerosol load. Atmos Chem Phys 2011; 11:10487 10501. doi:10.5194/acp-11-10487-2011.

Bond, T., Bergstrom, R.. Light absorption by carbonaceous parti- cles: An investigative review. Aerosol Sci Technol 2006;40(1):27 67. doi:10.1080/02786820500421521.

Bond, T.C., Doherty, S.J., Fahey, D.W., Forster, P.M., Berntsen, T., DeAngelo, B.J., Flanner, M.G., Ghan, S., K archer, B., Koch, D., Kinne, S., Kondo, Y., Quinn, P.K., Saro m, M.C., Schultz, M.G., Schulz, M., Venkataraman, C., Zhang, H., Zhang, S., Bellouin, N., Guttikunda, S.K., Hopke, P.K., Jacobson, M.Z., Kaiser, J.W., Klimont, Z., Lohmann, U., Schwarz, J.P., Shindell, D., Storelvmo, T., Warren, S.G., Zender, C.S.. Bounding the role of black carbon in the climate system: A scienti c assessment. J Geophys Res: Atmos 2013; 118:5380 5552. doi:10.1002/jgrd.50171-2013.

Boylan, J., Russel, A.. PM and light extinction model performance metrics, goals, and criteria for three dimensional air quality models. Atmos Env 2006; 40:4946 4959. doi: 10.1016/j.atmosenv.2005.09.087.

Briant, R., Tuccella, P., Deroubaix, A., Khvorostyanov, D., Menut, L., Mailler, S., Turquety, S.. Aerosol-radiation interaction modelling using online coupling between the wrf 3.7.1 meteorological model and the chimere 2016 chemistry-transport model, through the oasis3-mct coupler. Geosci Model Dev 2017;10:927 944. doi:10.5194/gmd-10-927-2017,2017.

Carlton, A., Pinder, R., Bhave, P., Pouliot, G.. What extent can biogenic SOA be controlled. Environ Sci Technol 2010; 9:3376 80. doi:10.1021/es903506b.

Chandra, S., Satheesh, S.K., Srinivasan, J.. Can the state of mixing of black carbon aerosols explain the mystery of excess atmospheric absorption? Geophys Res Lett 2004;31: L19109. doi:10.1029/2004GL020662.

Chrit, M., Sartelet, K., Sciare, J., Pey, J., Marchand, N., Couvidat, F., Sellegri, K., Beekmann, M.. Modelling organic aerosol concentrations and properties during ChArMEx summer campaigns of 2012 and 2013 in the western Mediterranean region. Atmos Chem Phys 2017; 17:12509 12531. doi:10.5194/acp-17-12509-2017.

Chylek, P., Coakley, J.. Aerosols and Climate. Science 1974; 183:75 77.

Couvidat, F., Debry, E., Sartelet, K., Seigneur, C.. A hydrophilic/hydrophobic organic (H^2O) aerosol model: Development,evaluation and sensitivity analysis. J Geophys Res 2012;117:D10304. doi:10.1029/211JDO17274.

Couvidat, F., Sartelet, K.. The Secondary Organic Aerosol Proces- sor (SOAP v1.0) model: a unified model with different ranges of com- plexity based on the molecular surrogate approach. Geosci Model Dev 2015;8:1111 1138. doi:10.5194/gmd-8-1111-2015.

Curci, G., Alyuz, U., Barò, R., Bianconi, R., Bieser, J., Christensen, J., Colette, A., Farrow, A., Francis, X., PedGuerrero, P.J., Im, U., Liu, P., Manders, A., L., P.P., Prank, M., Pozzoli, L., Sokhi, R., Solazzo, E., Tuccella, P., Unal, P., Vivanco, M., Hogrefe, C., Galmarini, S.. Modelling black carbon absorption of solar radiation. Atmos Chem Phys 2019;19:181 204. doi:10.5194/acp-19-181-2019.

Deboudt, K., Flament, P., Cho el, M., Gloter, A., Sobanska, S., Colliex, C.. Mixing state of aerosols and direct observation of carbonaceous and

marine coatings on African dust by individual particle analysis. J Geophys Res 2010;115: D24207. doi:10.1029/2010JD013921.

Debry, É., Fahey, K., Sartelet, K., Sportisse, B., Ahmed de Biasi, M., Tombette, M.. Technical Note: A new SIze REsolved Aerosol Model (SIREAM). Atmos Chem Phys 2007; 7:1537 1547. doi:10.5194/acp.7-1537-2007.

Dergaoui, H., Sartelet, K.N., Debry, E., Seigneur, C.. Model- ing coagulation of externally mixed particles: Sectional approach for both size and chemical composition. J Aerosol Sci 2013; 58:17 32. doi: 10.1016/j.jaerosci.2012.11.007.

Dey, S., Tripathi, S.N., Mishra, S.K.. Probable m i x i n g state of aerosols in the Indo-Gangetic Basin, northern India. Geophys Res Lett 2008;35: L03808. doi:10.1029/2007GL032622.

Emmons, L.K., Walters, S., Hess, P., Lamarque, J., P ster, G., Fillmore, D., Granier, C., Guenther, A., D. Kinnison, D., Laepple, T., Orlando, J., Tie, X., Tyndall, G., Wiedinmyer, C., Baughcum, S., Kloster, S.. Description and evaluation of the model for ozone and related chemical tracers, version 4 (mozart-4). Geosci Model Dev 2010; 3:43 67. doi:10.5194/gmd-3-43-2010.

Freney, E., Sellegri, K., Chrit, M., Adachi, K., Brito, J., Waked, A., Borbon, A., Colomb, A., Dupuy, R., Pichon, J.M., Bouvier, L., Delon, C., Jambert, C., Durand, P., Bourianne, T., Gaimoz, C., Triquet, S., Féron, A., Beekmann, M., Dulac, F., Sartelet, K.. Aerosol composition

and the contribution of SOA formation over Mediterranean forests. Atmos Chem Phys 2018; 18:7041 7056. doi:10.5194/acp-18-7041-2018.

Guenther, A., Karl, T., Harley, P., Wiedinmyer, C., Palmer, P., Geron, C.. Estimates of global terrestrial isoprene emissions using MEGAN (Model of Emissions of Gases and Aerosols from Nature). Atmos Chem Phys 2006; 6:3181 310. doi:10.5194/acp-6-3181-2006.

Gurci, G., Hogrefe, C., Bianconi, R., Im, U., Balzarini, A., Baró, R., Brunner, D., Forkel, R., Giordano, L., Hirtl, M., Honzak, L., Jiménez-Guerrero, P., Knote, C., Langer, M., Makar, P., Pirovano, G., Pérez, J., San José, R., Syrakov, D., Tuccella, P., Werhahn, J., Wolke, R., Zabkar, R., Zhang, J., Galmarini, S.. Uncertainties of simulated aerosol optical properties induced by assumptions on aerosol physical and chemical properties: An AQMEII-2 perspective. Atmos Env 2015; 115:541 55. doi: 10.1016/j.atmosenv.2014.09.009.

Guth, J., Josse, B., Marécal, V., Joly, M., Hamer, P.. First implementation of secondary inorganic aerosols in the MOCAGE version R2.15.0 chemistry transport model. Geosci Model Dev 2015; 9:137 160. doi:10.5194/gmd-9-137-2016.

Hansen, J . , Sato, H., Ruedy, R., Lacis, A., Asamoah, K., Beckford, K., Borenstein, S., Brown, E., Cairns, B., Carlson, B., Curran, B., de Castro, S., Druyan, L., Etwarrow, P., Ferede, T., Fox, M., Ga en, D., Glascoe, J., Gordon, H., Hollandsworth, S., Jiang, X., Johnson, C., Lawrence, N., Lean, J., Lerner, J., Lo, K., Logan, J., Luckett, A., McCormick, M., McPeters, R., Miller, R.L., Minnis, P., Ramberran, I.,

Russell, G., Russell, P., Stone, P., Tegen, I., Thomas, S., Thomason, L., Thompson, A., Wilder, J., Willson, R., Zawodn, J.. Forcings and chaos in inter annual to decadal climate change. J Geophys Res 1997; 102:25679 25720. doi:10.1029/97JD01495.

Haywood, J., Boucher, O.. Estimates of the direct and indirect radiative forcing due to tropospheric aerosols: A review. Rev Geophys 2000;38:513 543. doi:10.1029/1999RG000078.

Healy, R., Sciare, J., Poulain, L., Kamili, K., Merkel, M., M uller, T., Wiedensohler, A., Eckhardt, S., Stohl, A., Sarda-Estève, R., McGillicuddy, E., O'Connor, I., Sodeau, J., Wenger, J.. Sources and mixing state of size-resolved elemental carbon particles in a European megacity: Paris. Atmos Chem Phys 2012; 12:1681 1700. doi:10.5194/acp- 12-1681-2012.

Hess, M., Koepke, P., Schult, I.. Optical properties of aerosols and clouds: The software package OPAC. B Am Meteorol Soc 1998; 79:831 844. doi:10.1175/1520-0477(1998)079<0831.

Holben, B., Eck, T., Slutsker, I., Tanré, D., Buis, J., Setzer, A., Vermote, E., Reagan, J., Kaufman, Y., Nakajima, T., Lavenu, F., Jankowiak, I., Smirnov, A.. AERONET : A federated instrument network and data archive for aerosol characterization. Remote Sens Environ 1998;66:1 16. doi:10.1016/S0034-4257(98)00031-5.

Holben, B., Tanre, D., Smirnov, A., Eck, T.F., Slutsker, I., Abuhassan, N., Newcomb, W.W., Schafer, J., Chatenet, B., Lavenu, F., Kaufman,

Y.J., Vande Castle, J., Setzer, A., Markham, B., Clark, D., Frouin, R., Halthore, R., Karnieli, A., O'Neill, N.T., Pietras, C., Pinker, R.T., Voss, K., Zibordi, G.. An emerging ground-based aerosol climatology: Aerosol Optical Depth from AERONET. J Geophys Res 2001;106:12067 12097. doi:10.1029/2001JD900014.

Jacobson, M.. Control of fossil fuel particulate black carbon and organic matter, possibly the most effective method of slowing global warming. J Geophys Res: Atmos 2002;107: ACH 16 1 ACH 16 22. doi:10.1029/2001JD001376.

Jacobson, M., Hansson, H., Noone, K.J., Charlson, R.. Organic atmospheric aerosols: Review and state of the science. Rev Geophys 2000; 38:267 294. doi:10.1029/1998RG000045.

Jacobson, M., Turco, R., Jensen E.J.and Toon, O.. Modeling coagulation among particles of different composition and size. Atmos Env 1994; 28:1327 1338. doi:10.1016/1352-2310(94)90280-1.

Jacobson, M.Z.. Strong radiative heating due to the mixing state of black carbon in atmospheric aerosols. Nature 2001;409(695-697).

Khalizov, A., Xue, H., Zhang, R.. Enhanced light absorption and scattering by carbon soot aerosols internally mixed with sulfuric acid. J Phys Chem 2009; 113:1066 1074. doi:10.1021/jp807531n.

Kim, Y., Couvidat, F., Sartelet, K., Seigneur, C.. Comparison of Different Gas-Phase Mechanisms and Aerosol Modules for Simulating Par-

ticulate Matter Formation. J Air Waste Manage 2011; 61:11:1218 1226. doi:10.1080/10473289.2011.603999.

Kleeman, M.J., Cass, G.R.. A 3D Eulerian source-oriented model for an externally mixed aerosol. Environ Sci Technol 2001; 35:4834 4848. doi:10.1021/es010886m.

Kleeman, M.J., Cass, G.R., Eldering, A.. Modeling the airborne particle complex as a source-oriented external mixture. J Geophys Res: Atmos 1997; 102:21355 21372. doi:10.1029/97JD01261.

Klingmuller, K., Steil, B., Br uh, C., Tost H.and Lelieveld, J.. Sensitivity of aerosol radiative effects to different mixing assumptions in the AEROPT 1.0 submodel of the EMAC atmospheric-chemistry-climate model. Geosci Model Dev 2014; 7:2503 2516. doi:10.5194/gmd-7-2503-2014.

Koehler, K., DeMott, P., Kreidenweis, S., Popovicheva, O., Petters, M., Carrico, C., Kireev, E., Khokhlova, T., Shonija, N.. Cloud condensation nuclei and ice nucleation activity of hydrophobic and hydrophilic soot particles. Phys Chem Chem Phys 2009;36:7906 20. doi:10.1039/b905334b.

Lack, D.A., Langridge, J.M., Bahreini, R., Cappa, C.D., Middlebrook, A.M., Schwarz, J.. Brown carbon and internal mixing in biomass burning particles. Proc Natl Acad Sci 2012;109:14802 14807. doi:10.1073/pnas.1206575109.

Lesins, G., Chylek, P., Lohmann, U.. A study of internal and external mixing scenarios and its effect on aerosol optical properties and direct radiative forcing. J Geophys Res 2002;107(D10): 4094. doi:10.1029/doi:10.1029/2001JD000973.

Li, Y.P., Elbern, H., Lu, K.D., Friese, E., Kiendler-Scharr, A., Mentel, T.F., Wang, X.S., Wahner, A., Zhang, Y.H.Z.. Updated aerosol module and its application to simulate secondary organic aerosols during impact campaign may 2008. Atmos Chem Phys 2015; 13:6289 6304. doi:10.5194/acp-13-6289-2013.

Lu, J., Bowman, F.. A detailed aerosol mixing state model for investigating interactions between mixing state, semi volatile partitioning, and coagulation. Atmos Chem Phys 2010; 10:4033 4046. doi:10.5194/acp-10-4033-2010.

Majdi, M., Turquety, S., Sartelet, K., Legorgeu, C., Menut, L., Kim, Y.. Impact of wildfires on particulate matter in the Euro-Mediterranean in 2007: sensitivity to the parameterization of emissions in air quality models. Atmos Chem Phys 2019; 19:785 812. doi:10.5194/acp-19-785-2019.

Mallet, V., Quélo, D., Sportisse, B., Ahmed de Biasi, M., Debry, É., Korsakissok, I., Wu L.and Roustan, Y., Sartelet, K., Tombette, M., Foudhil, H.. Technical Note: The air quality modeling system Polyphemus. Atmos Chem Phys 2007; 7:5479 5487. doi:10.5194/acp-7-6459-2007.

Matsui, H., Hamilton, D., Mahowald, N.M.. Black carbon radiative effects highly sensitive to emitted particle size when resolving mixing-state diversity. Nat Commun 2018; 9:2041 1723. doi:10.1038/s41467-018-05635-1.

Maxwell Garnett, J.C.. Colours in metal glasses and metal lms. Philosophical Transactions of the Royal Society A 1904; 3:385 420.

Menut, L., Perez Garcia-Pando, C., Haustein, K., Bessagnet, B., Prigent, C., Alfaro, S.. Relative impact of roughness and soil texture on mineral dust emission fluxes modeling. J Geophys Res: Atmos 2013; 118:6505 6520. doi:10.1002/jgrd.50313.

Mie, G.. Beiträge zur Optik trüber Medien, speziell kolloidaler Metallösungen. Ann Phys 1908;330:377 445. doi:10.1002/andp.19083300302.

Mishenko, M., Goegdzhayev, I., Cairns, B., Rossow, W., Lacis, A.. Aerosol retrievals over the ocean by use of channels 1 and 2 AVHRR data: sensitivity analysis and preliminary results. Appl Optics 1999; 38:7325 7341. doi:10.1364/AO.38.007325.

Monahan, E.C.. In The Role of Air-Sea Exchange in Geochemical Cycling; Kluwer Academic Publishers. p. 129 163.

Monks, P., Granier, C., Fuzzi, S., Stohl, A., Williams, M., Akimoto, H., Amann, M., Baklanov, A., Baltensperger, U., Bey, I., Blake, N., Blake, R., Carslaw, K., Cooper, O., Dentener, F., Fowler, D., Fragkou, E., Frost, G., Generoso, S., Ginoux, P., Grewe, V., Guenther, A., Hansson, H., Henne, S., Hjorth, J., Hofzumahaus, A., Huntrieser, H., Isaksen, I., Jenkin, M., Kaiser, J., Kanakidou, M., Klimont, Z., Kulmala, M., Laj, P., Lawrence, M., Lee, J., Liousse, C., Maione, M., McFiggans, G., Metzger, A., Mieville, A., Moussiopoulos, N., Orlando, J., O'Dowd, C., Palmer, P., Parrish, D., Petzold, A., Platt, U., P Oschl, U., Prévôt, A., Reeves, C., Reimann, S., Rudich, Y., Sellegri, K., Steinbrecher, R., Simpson, D., ten Brink, H., Theloke, J., Van der Werf, G., Vautard, R., Vestreng, V., Vlachokostas, C., von Glasow, R..

Atmospheric composition change - global and regional air quality. Atmos Env 2009;43:5268 5350. doi: 10.1016/j.atmosenv.2009.08.021.

Nabat, P., Somot, S., Mallet, M., Michou, M., Sevault, F., Driouech, F., Meloni, D., di Sarra, A., Di Biagio, C., Formenti, P., Sicard, M., LÉon, J.F., Bouin, M.N. Dust aerosol radiative effects during summer 2012 simulated with a coupled regional aerosol-atmosphere-ocean model over the Mediterranean. Atmos Chem Phys 2015; 15:3303 3326. doi:10.5194/acp- 15-3303-2015.

Nenes, A., Pilinis, C., Pandis, S. ISORROPIA: A new thermodynamic model for inorganic multicomponent atmospheric aerosols. Aquat Geochem 1998; 4:123 152. doi:10.1023/A:1009604003981.

Oshima, N., Koike, M., Zhang, Y., Kondo, Y., Moteki, N., Takegawa, N., Miyazaki, Y.. Aging of black carbon in outflow from anthropogenic sources using a mixing state resolved model: Model development and evaluations. J Geophys Res 2009;114: D06210. doi:10.1029/2008JD010680.

Pascal, M., Corso, M., Chanel, O., Declercq, C., Badaloni, C., Ce- saroni, G., Henschel, S., Meister, K., Haluza, D., Martin-Olmedo, P., Medinaa, S., on behalf of the Aphekom group, . Assessing the public health impacts of urban air pollution in 25 European cities: Results of the Aphekom project. Sci Total Environ 2013; 449:390 400. doi: 10.1016/j.scitotenv.2013.01.077.

Péré, J.C., Bessagnet, B., Mallet, M., Waquet, F., Chiapello, I., Minvielle, F., Pont V.and Menut, L.. Direct radiative effect of the russian wild res

and its impact on air temperature and atmospheric dynamics during august 2010. Atmos Chem Phys 2014;14:1999 2013. doi:10.5194/acp-14-1999-2014.

Rea, G., Turquety, S., Menut, L., Briant, R., Mailler, S., Siour, G.. Source contributions to 2012 summertime aerosols in the Euro-Mediterranean region. Atmos Chem Phys 2015;15(14):8013 8036. doi:10.5194/acp-15-8013-2015.

Riemer, N., Ault, A.P., Craig, R.L., Curtis, J.H., West, M.. Aerosol mixing state: Measurements, modeling, and impacts. Rev Geophys 2019; doi:10.1029/2018RG000615.

Sartelet, K., Couvidat, F., Seigneur, C., Roustan, Y.. Impact of biogenic emissions on air quality over Europe and North America. Atmos Env 2012; 53:131 141. doi: 10.1016/j.atmosenv.2011.10.046.

Satheesh, S.K., Srinivasan, J., Moorthy, K.K. Spatial and temporal heterogeneity in aerosol properties and radiative forcing over Bay of Bengal: Sources and role of aerosol transport. J Geophys Res 2006;111: D08202. doi:10.1029/2005JD006374.

Tombette, M., Chazette, P., Sportisse, B., Roustan, Y.. Simulation of aerosol optical properties over Europe with a 3-D size-resolved aerosol model: Comparisons with AERONET data. Atmos Chem Phys 2008; 8:7115 7132. doi:10.5194/acp-8-7115-2008.

Turquety, S., Menut, L., Bessagnet, B., Anav, A., Viovy, N., Maignan, F., Wooster, M.. APIFLAME v1.0: high resolution re emission model

and application to the Euro-Mediterranean region. Geosci Model Dev 2014; 7:587 612. doi:10.5194/gmd-7-587-2014.

Twomey, S.. The Influence of Pollution on the Shortwave Albedo of Clouds. J Atmospheric Sci 1977; 34:1149 1154. doi:10.1175/1520-0469.

Yarwood, G., Rao, S., Yocke, M., Whitten, G.. Updates to the carbon bond chemical mechanism: CB05 Final report to the US EPA 2005.

Zhu, S., Sartelet, K., Healy, R., Wenger, J.. Simulation of particle di- versity and mixing state over Greater Paris: A model- measurement inter-comparison. Faraday Discuss 2016; 189:547 566. doi:10.1039/C5fd00175g.

Zhu, S., Sartelet, K., Seigneur, C.. A size-composition resolved aerosol model for simulating the dynamics of externally mixed particles: SCRAM (v 1.0). Geosci Model Dev 2015; 8:1595 1612. doi:10.5194/gmd-8-1595- 2015.

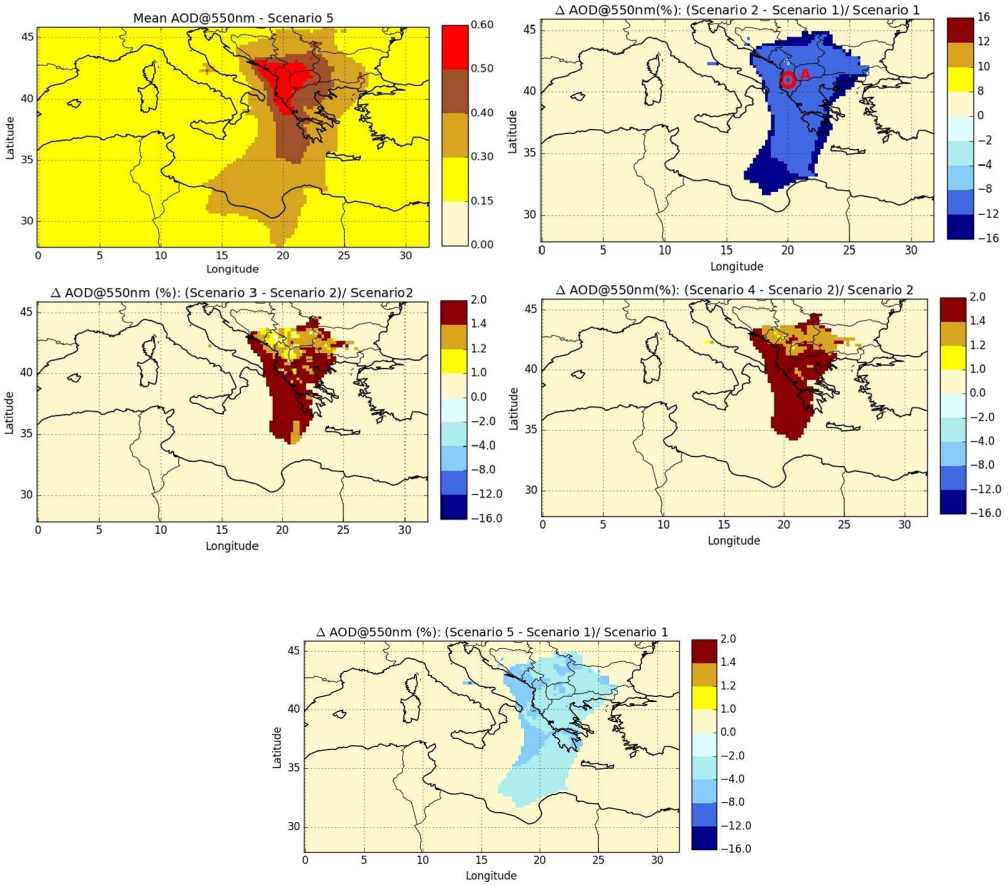

Figure 3: Mean AOD at 550 nm (left upper panel) from scenario 5 (Majdi et al., 2019) and sensitivity of AOD at 550 nm to the mixing-state scenario (right upper panel: relative difference between scenarios 2 and 1, left middle panel: relative difference between scenarios 3 and 2, and right middle panel: relative difference between scenarios 4 and 2), to the core-shell representation (lower panel: relative difference between scenario 5 and scenario 1) over the Euro-Mediterranean region between 20 and 31 July 2007. The red point A (in upper left panel) represents the location where the extinction coefficient (β_{ext}) is evaluated for each scenario.

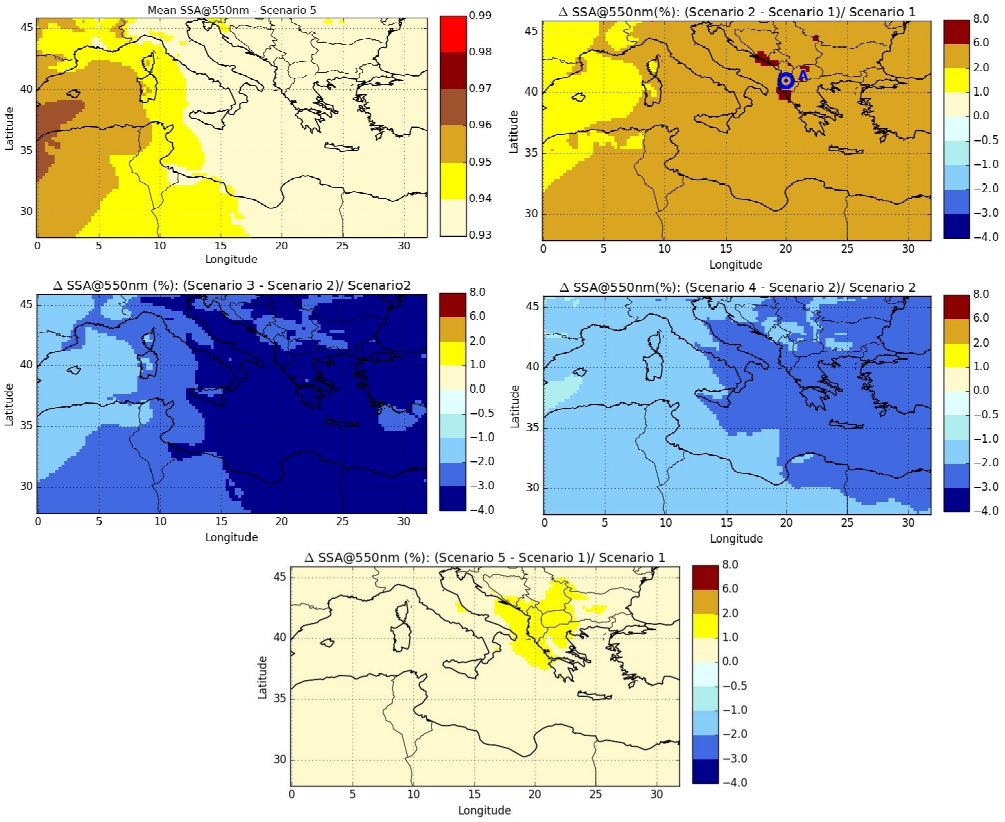

Figure 4: Mean SSA at 550 nm (left upper panel) from scenario 5 (Majdi et al., 2019) and sensitivity of SSA at 550 nm to the mixing-state scenario (right upper panel: relative difference between scenarios 2 and 1, left middle panel: relative difference between scenarios 3 and 2, and right middle panel: relative difference between scenarios 4 and 2), to the core-shell representation (lower panel: relative difference between scenario 5 and scenario1) over the Euro-Mediterranean region between 20 and 31 July 2007. The blue point A (in upper left panel) represents the location where the backscattering coefficient (β_{sca}) is evaluated for each scenario.

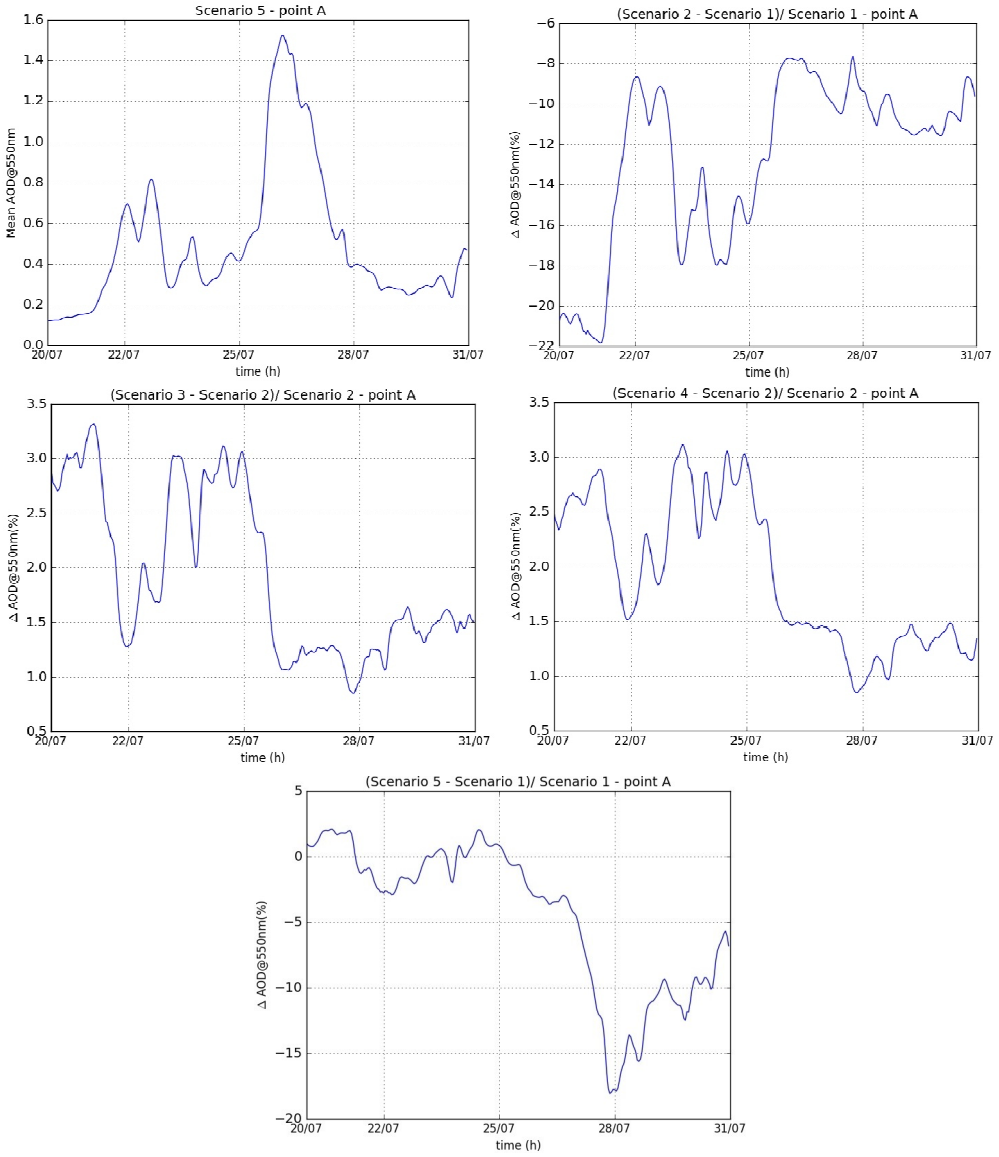

Figure 5: Time evolution of AOD at 550 nm (left upper panel) from scenario 5 (Majdi et al., 2019) and sensitivity of AOD at 550 nm to the mixing-state scenario (right upper panel: hourly relative difference between scenarios 2 and 1, left middle panel: hourly relative difference between scenarios 3 and 2, and right middle panel: hourly relative difference between scenarios 4 and 2), to the core-shell representation (lower panel: hourly relative difference between scenario 5 and scenario 1) at point A between 20 and 31 July 2007.

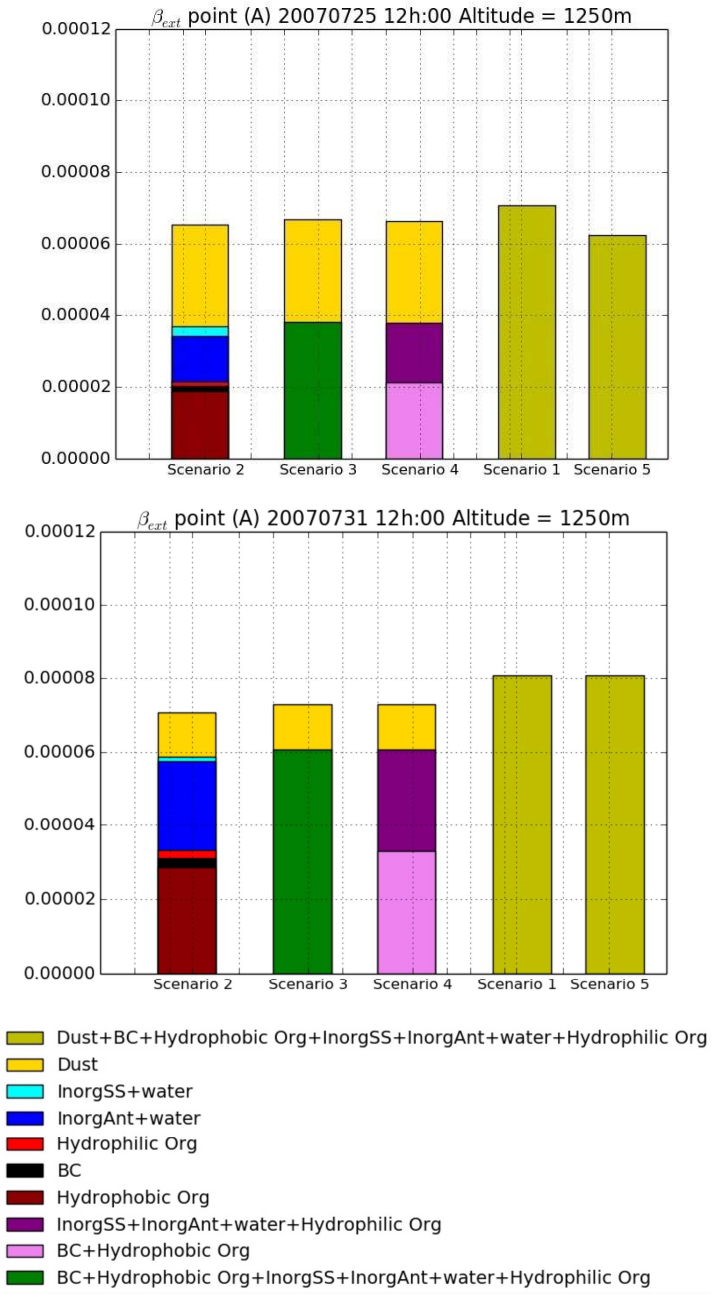

Figure 6: Extinction coefficient (β_{ext}) for the different scenarios and particle types on 25 July 2007 (upper panel) and 31 July 2007 (lower panel) at midday and at the vertical level of 1250 m at point A.

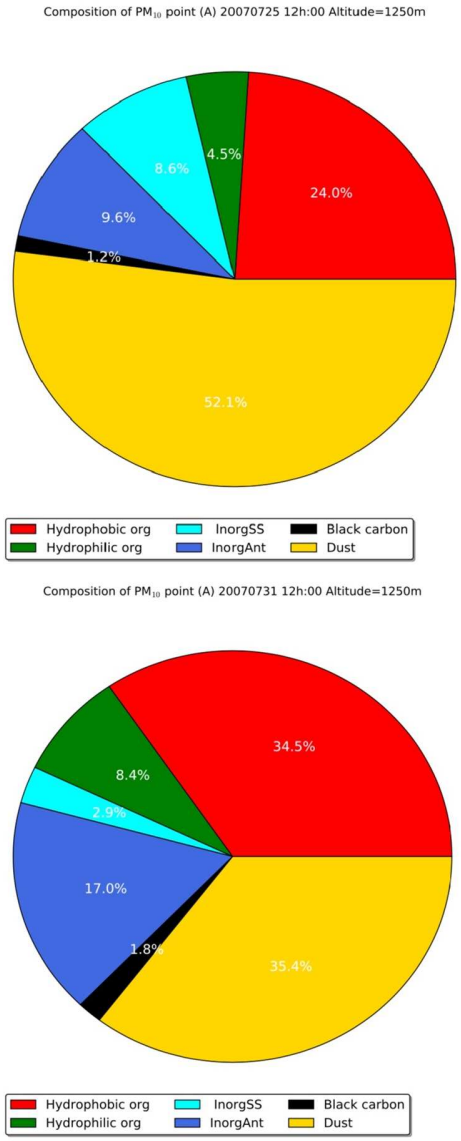

Figure 7: Composition of PM_{10} on 25 July 2007 (left panel) and 31 July 2007 (right panel) at midday and at the vertical level of 1250 m at point A.

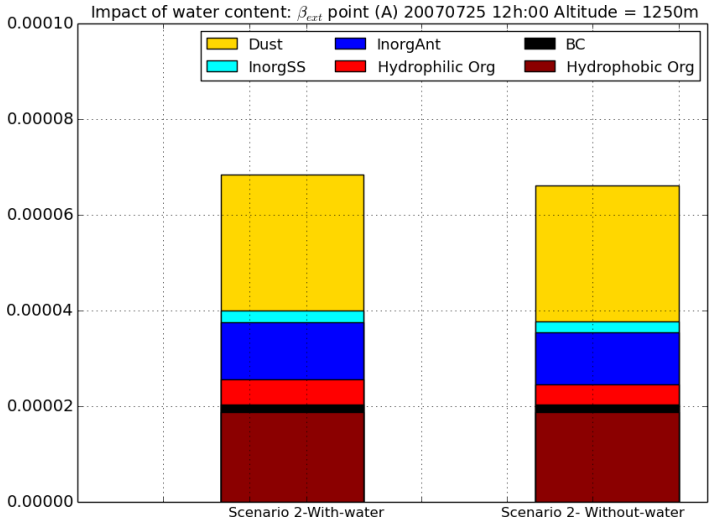

Figure 8: Extinction coefficient (β_{ext}) for scenarios 2-with-water and scenarios 2-without- water, for each particle types on 25 July 2007 at midday and at the vertical level of 1250 m at point A.